Temporal and Spatial Variation in Growth Condition of Pacific Salmon

Hiromichi Ueno[1], Masahide Kaeriyama[1], Moeko Otani[1], Mitsuho Oe[1], Yuxue Qin[1], Maki N. Aita[2], Seokjin Yoon[1], and Michio J. Kishi[1]

[1]Hokkaido University, 3-1-1 Minato-cho, Hakodate, Hokkaido 040-8611, Japan
[2]Japan Agency for Marine-Earth Science and Technology (JAMSTEC), 3173-25 Showa-machi, Kanazawa-ku, Yokohama 236-0001, Japan

Ueno, H., M. Kaeriyama, M. Otani, M. Oe, Y. Qin, M.N. Aita, S. Yoon, and M.J. Kishi. 2016. Temporal and spatial variation in growth condition of Pacific salmon. N. Pac. Anadr. Fish Comm. Bull. 6: 181–187. doi:10.23849/npafcb6/181.187.

Abstract: Temporal and spatial variation in the growth condition of Pacific salmon (*Oncorhynchus* spp.) were investigated using the prey-density function for consumption. Zooplankton prey density was estimated from an ecosystem model, NEMURO, embedded in a 3D physical model for the years 1948–2007. This study focused on three species of Pacific salmon (chum (*O. keta*), pink (*O. gorbuscha*), and sockeye (*O. nerka*)), all of which are zooplankton feeders. The prey dependence function for consumption of Pacific salmon varies on a decadal time scale, and its empirical orthogonal function first mode was correlated with the Pacific Decadal Oscillation. The variation in the prey dependence function for consumption in the Bering Sea and the Western Subarctic Gyre was correlated with the variation in the carrying capacity of chum, pink, and sockeye salmon, indicating that these are key areas for connecting climate variability to the carrying capacity of Pacific salmon. In these areas, prey density increased after the 1976/77 regime shift, in synchrony with the increase in primary production due to enhanced nutrient supply through deepening of the mixed layer and/or stronger Ekman upwelling.

Keywords: Pacific salmon, 3D NEMURO, prey density, empirical orthogonal function, growth

INTRODUCTION

Pacific salmon (*Oncorhynchus* spp.) play an essential role in the North Pacific ecosystem and in addition are a substantial fishery resource. Pacific salmon also have a significant role in the biodiversity and productivity of riparian ecosystems because they supply marine-derived nutrients to rivers (e.g., Kaeriyama and Minagawa 2008). The dominant species of Pacific salmon are chum (*O. keta*), pink (*O. gorbuscha*), and sockeye (*O. nerka*), which together account for about 90% of the commercial catch in the North Pacific (e.g., Irvine et al. 2013). We focused on these three dominant species in this study.

Kaeriyama et al. (2009) estimated the carrying capacity of chum, pink, and sockeye salmon in the North Pacific, defined as the replacement level of Ricker's recruitment curve, and found that their carrying capacity was synchronous with climate variability as indicated by, for example, the strength of the Aleutian Low. Kaeriyama et al. (2009) also estimated the Ricker stock-recruitment equilibrium level from brood tables based on expanded catch data. This equilibrium point is a measure of the production capacity of the species at the gross scale of the North Pacific and provides an index of the carrying capacity for each salmon species. The time span of data used to estimate the carrying capacity for year class, t, is 20 brood years for sockeye and chum salmon from year class t to $t + 20$, and 10 generations of odd- and even-year groups for pink salmon. The carrying capacity of the three species (chum, pink, and sockeye salmon) was low during the 1945–1955 year classes, increased during the 1956–1975 year classes, and remained constant during the 1976–1996 year classes. This inter-decadal variation mostly corresponds to climate indices such as the Aleutian Low Pressure Index (ALPI, Beamish and Bouillion 1993) and the Pacific Decadal Oscillation (PDO, Mantua et al. 1997).

The relationship between large-scale climate variability and salmon production has been studied from various perspectives. In the Gulf of Alaska, a strong Aleutian Low (positive ALPI) is suggested to induce strong freshwater discharge, low sea surface salinity, strong stratification (e.g., Gargett 1997; Royer et al. 2001), a shallow winter mixed layer (e.g., Polovina et al. 1995), good light conditions, high zooplankton production (e.g., Brodeur et al. 1996), and high salmon production (e.g., Hare et al. 1999). However, due to the lack of long-term, wide-ranging data, the detailed processes connecting climate variability and salmon production

All correspondence should be addressed to H. Ueno.
e-mail: ueno@fish.hokudai.ac.jp

are not clear. In this study, we aim to provide a better understanding of the relationship between climate variability and the carrying capacity of Pacific salmon from the perspective of prey density, statistically analyzing the output of a numerical model.

Kamezawa et al. (2007) and Kishi et al. (2010) investigated the effect of climate variability on the growth of Japanese chum salmon using a bioenergetics model coupled with a 3D lower trophic ecosystem model (3D North Pacific Ecosystem Model for Understanding Regional Oceanography (3D NEMURO; Aita et al. 2007)) assuming a migration route of Japanese chum salmon. They found that the prey density, especially in the eastern North Pacific, had a greater influence on the change in body size than did the sea surface temperature (SST) using 3D NEMURO. The present study investigates the temporal and spatial variation in prey density for chum, pink, and sockeye salmon through an empirical orthogonal function (EOF) analysis without assuming a migration route. We further try to understand the key areas for the variability in the growth of Pacific salmon and what determines the prey density variability in these key areas, considering the variation in primary production, mixed layer depth, and Ekman pumping.

MATERIALS AND METHODS

In this study, we assumed that the growth rate of an individual Pacific salmon is represented by the wet weight increment per day:

$$\frac{dW}{dt} = [C - (R + S + F + E)] \bullet \frac{CAL_z}{CAL_f} \bullet W. \quad (1)$$

This bioenergetics model follows Rudstam (1988), Ware (1978), Beauchamp et al. (1989), and Trudel et al. (2004) and was modified by Kamezawa et al. (2007) and Kishi et al. (2010). W is the wet weight of fish (g wet weight; g WW or g fish), C is consumption (g prey (g fish)$^{-1}$ d^{-1}), R is respiration or losses through metabolism (g prey (g fish)$^{-1}$ d^{-1}), S is specific dynamic action or losses due to the energy costs of digesting food (g prey (g fish)$^{-1}$ d^{-1}), F is egestion or losses in feces (g prey (g fish)$^{-1}$ d^{-1}), E is excretion or losses of nitrogenous excretory wastes (g prey (g fish)$^{-1}$ d^{-1}), and CAL_z and CAL_f are the caloric equivalents of prey (i.e., zooplankton) (cal (g prey)$^{-1}$) and fish (cal (g fish)$^{-1}$), respectively.

The growth of Pacific salmon is affected by climate variability, primarily through the consumption rate (C). C is estimated as the proportion of the maximum daily rations for Pacific salmon at a particular mass and temperature (Beauchamp et al. 1989; Megrey et al. 2002; Ito et al. 2004):

$$C = C_{MAX} \bullet \rho \bullet f_c(T) \quad (2)$$

$$C_{MAX} = ac \bullet W^{bc}, \quad (3)$$

where C_{MAX} is the maximum consumption rate (g prey (g fish)$^{-1}$ d^{-1}), ρ (no dimension) is the available consumption rate without temperature effects (prey dependence function for consumption), $f_c(T)$ (no dimension) is a temperature dependence function for consumption formulated by Thornton and Lessem (1978), T is water temperature (°C), ac is the intercept of the mass dependence function for 1 g WW at the optimum water temperature (set to be a constant, 0.303), and bc is the coefficient of mass dependence (set to be a constant, -0.275; Beauchamp et al. 1989).

C can be affected by climate variability through the two components, ρ and $f_c(T)$, because C_{MAX} is constant. As mentioned in the previous section, this study focused on ρ, which was determined by prey density. This is because the relationship between temperature variation and salmon production has been studied in detail through analyses of long-term, wide-ranging sea surface temperature data (e.g., Mantua et al. 1997; Stachura et al. 2014). ρ is determined as follows (Fig. 1):

$$\rho = \frac{\frac{PD \bullet V_i}{K_i}}{1 + \frac{PD \bullet V_i}{K_i}}, \quad (4)$$

where PD is the density of prey (g wet weight m^{-3} or g prey m^{-3}), V_i is the vulnerability at stage i (no dimension) and is set to be a constant (1.0), and K_i is the half-saturation constant (g prey m^{-3}) and set to be 0.15 (Kamezawa et al. 2007; Kishi et al. 2010). The formulations for the individual processes described above were the same as those used in Kamezawa et al. (2007), Kishi et al. (2010), and Yoon et al. (2015).

The prey density in our bioenergetics model was obtained from Aita et al. (2007), who calculated a 3D physical-ecological coupled model (3D NEMURO) for the northern Pacific from 1948 to 2007 (extended by 5 years from the original dataset of 1948–2002 in Aita et al. (2007)). We used the monthly averaged output (temperature and density of predatory zooplankton) for the upper 20 m of the water col-

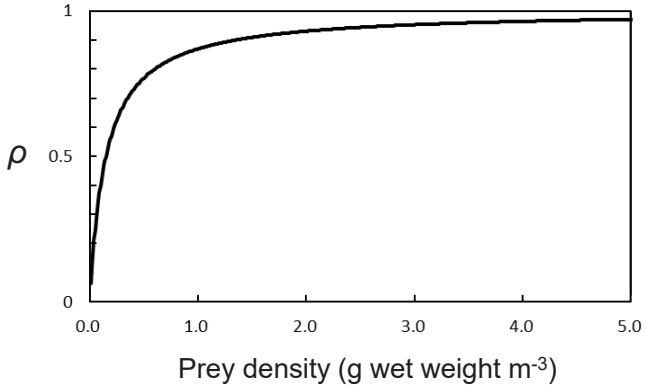

Fig. 1. The relationship between prey density and ρ (the prey density dependence function for consumption).

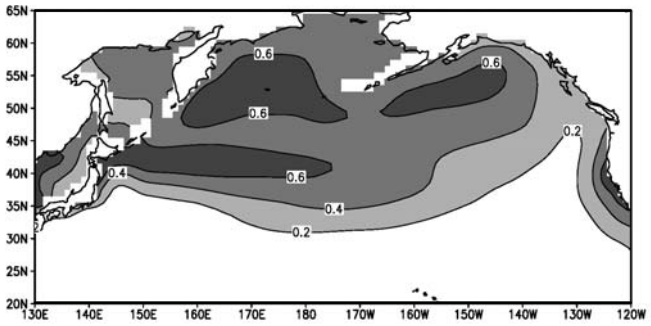

Fig. 2. Horizontal distribution of annual-mean ρ averaged over the analysis period (1948–2007).

umn at each 1° × 1° horizontal grid. We assumed predatory zooplankton (ZP), including jellyfish, salps, and/or krill (Kishi et al. 2007) to be prey, as indicated by previous studies of chum salmon (Kamezawa et al. 2007; Kishi et al. 2010; Yoon et al. 2015). In NEMURO, ZP density is described as the total amount of nitrogen per liter (mol N l^{-1}). In this study, we converted it into wet weight following Megrey et al. (2002):

$$\frac{14\ \mu g\ N}{\mu\ mole\ N} \bullet \frac{10^{-6}\ g}{\mu g} \bullet \frac{1\ g\ dw}{0.07\ g\ N\ dw} \bullet \frac{1\ g\ ww}{0.2\ g\ dw} \bullet \frac{10^{3}\ L}{m^{3}}, \quad (5)$$

where *dw* = dry weight and *ww* = wet weight. In the present study we used the following ZP:

$$ZP = ZP(NEMURO) \bullet 1.937 \quad (6)$$

because the ZP in NEMURO is smaller than the observed one by a factor of 1.937 as indicated by Kamezawa et al. (2007) and Kishi et al. (2010).

Figure 2 shows the annual mean climatological (averaged for 1948–2007) horizontal distribution of ρ derived through the procedure described above. ρ is relatively high in the subarctic North Pacific (north of about 40°N) and close to zero in the subtropical North Pacific (south of about 40°N). The EOF analysis (principal component analysis) was applied for monthly 1° x 1° ρ anomaly in the North Pacific north of 40°N during 1948–2007. EOF analysis is a principal component analysis frequently used in the study of climate variability. We set the analysis area to be north of 40°N because Pacific salmon are usually distributed there (e.g., Myers et al. 2007). The ρ anomaly used for EOF analysis was calculated through the following procedure to remove the effect of global warming. (1) Monthly ρ time-averaged over the analysis period in each 1° x 1° horizontal grid was subtracted from the ρ on a 1° x 1° grid (named ρ-anomaly-1). Then, (2) the horizontally averaged ρ-anomaly-1 over the analysis area in each month was subtracted from ρ-anomaly-1.

To compare the temporal variation in carrying capacity with that of ρ, we applied 24-year running means for 1975–1998, starting with the year. For example, 1975–1998 running mean was applied for the 1975 year class. This is because the carrying capacity in "*t*" year (e.g. 1975) was estimated using catch data from year class *t* to *t* + 20 (e.g. 1975 to 1995), and also because the *t* to *t* + 20 (e.g. 1975 to 1995) year classes actually experience the marine environment from *t* to *t* + 20 + 3 years (e.g. 1975 to 1998), considering their lifespan. For the 1985–1996 year classes, the time span for the running mean is < 24 years.

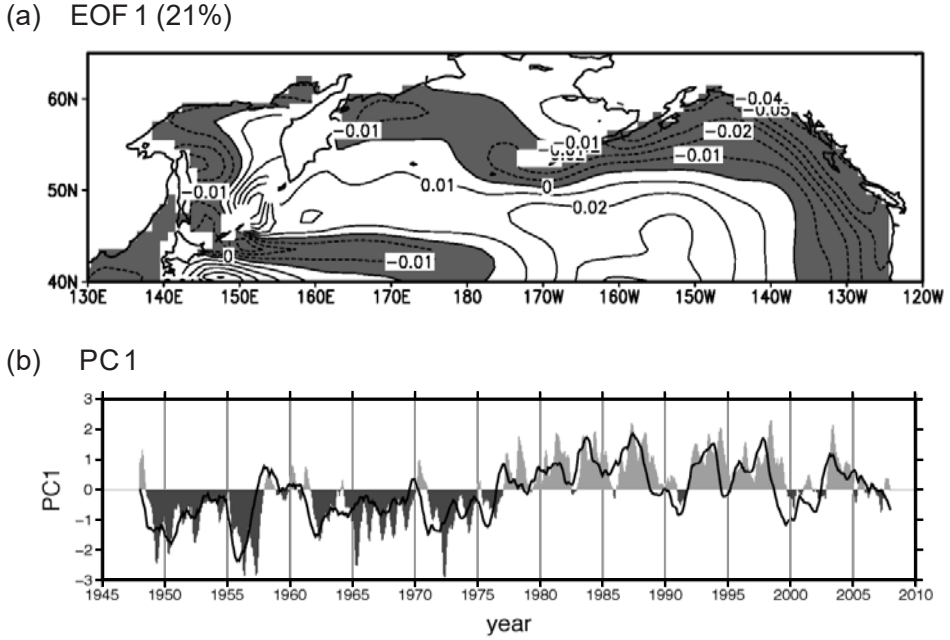

Fig. 3. (a) Spatial pattern and (b) the time coefficient of the EOF first mode. Solid line in (b) indicates the PDO index (http://research.jisao.washington.edu/pdo/) with a 13-month running mean filter.

RESULTS

The EOF first mode (the first principal component (PC1)) for the monthly 1° × 1° ρ anomaly explained 21.0% of the total variance (Fig. 3). The second mode explained 13.7% of total variance. The spatial structure of the EOF first mode has a negative peak in coastal Gulf of Alaska and a positive peak in the central eastern subarctic North Pacific (145°–170W°, 40°–50°N; Fig. 3a). The temporal coefficient of the EOF first mode (PC1) changed on an inter-decadal time scale and was mostly negative before 1976 and mostly positive after 1977 (Fig. 3b). This time variation was correlated with that of the PDO index (solid line in Fig. 3b: the correlation coefficient was 0.72, significant at the 99% confidence level). In addition, the spatial structure of the EOF first mode was similar to the spatial structure of the PDO (see http://research.jisao.washington.edu/pdo/) except in the area east of Hokkaido, Japan (145°E–180°, 42°–45°N), where the ecosystem is not reproduced well by 3D NEMURO due to the low resolution of the physical model (Aita et al. 2007). Therefore, it is likely that the growth condition of Pacific salmon changes inter-decadally in correlation with the PDO.

Based on the ρ distribution averaged over the time period 1948–2007 (Fig. 2) and the spatial structure of the EOF first mode (Fig. 3a), we selected five key areas for the growth of Pacific salmon: the Bering Sea shelf (BS-S), Bering Sea basin (BS-B), Western Subarctic Gyre (WSAG), central eastern subarctic North Pacific (CE-SNP), and coastal Gulf of Alaska (C-GoA; Fig. 4a). In the BS-S and BS-B, the ρ anomaly changed decadally. The most prominent change occurred in 1976/77, with the ρ anomaly mostly negative (prey density was below average) before 1976/77 and mostly positive (prey density was above average) after that time (Fig. 4b, c). In the WSAG (Fig. 4d) the ρ anomaly was mostly negative before the mid-1970s and mostly positive after that time in summer and winter. In contrast, the ρ anomaly was mostly positive before 1976/77 and mostly negative after that time in the C-GoA (Fig. 4f) and did not show any distinct long-term variation in the CE-SNP (Fig. 4e).

The carrying capacity of chum, pink, and sockeye salmon, whose variation mechanism is the main objective of this study, was low before the 1955 year class, increased during the 1956–1975 year classes, and remained constant after the 1976 year class (Fig. 5a). This temporal variation was consistent with the variations in ρ in the areas of BS-S, BS-B, and WSAG, where the prey density increased from the mid-1950 to the mid-1970 year classes (Fig. 5b, c and d). The correlation coefficients were 0.75, 0.77 and 0.69 in BS-S, BS-B, and WSAG in summer and 0.67 in WSAG in winter (significant at the 99% confidence level). In contrast, in the C-GoA, the ρ decreased before the mid-1970 year classes and remained constant in summer and winter, which was inconsistent with the temporal change in carrying capacity. In the CE-SNP, the ρ was high during the 1960–1980 year classes in summer and winter, also inconsistent with the change in carrying capacity. These results suggest that the

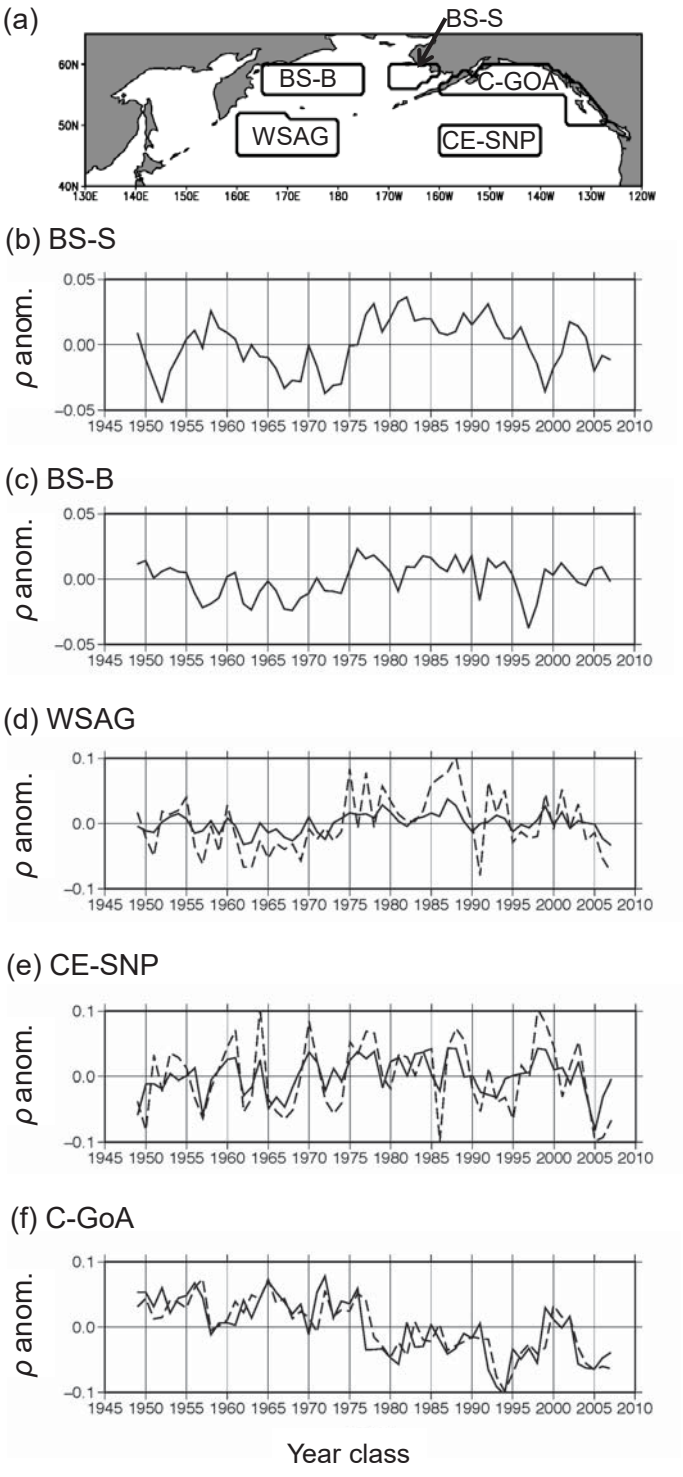

Fig. 4. (a) Schematic view of five key areas and the interannual variation of the ρ anomaly in summer (June–October, solid line) and winter (December–April, dashed line) in (b) the Bering Sea shelf (BS-S), (c) Bering Sea basin (BS-B), (d) Western Subarctic Gyre (WSAG), (e) central eastern subarctic North Pacific (CE-SNP), and (f) coastal Gulf of Alaska (C-GoA). Mean values are (b) 0.59, (c) 0.67, (d) 0.61, (e) 0.52, and (f) 0.46 in summer, and (d) 0.58, (e) 0.46, and (f) 0.37 in winter.

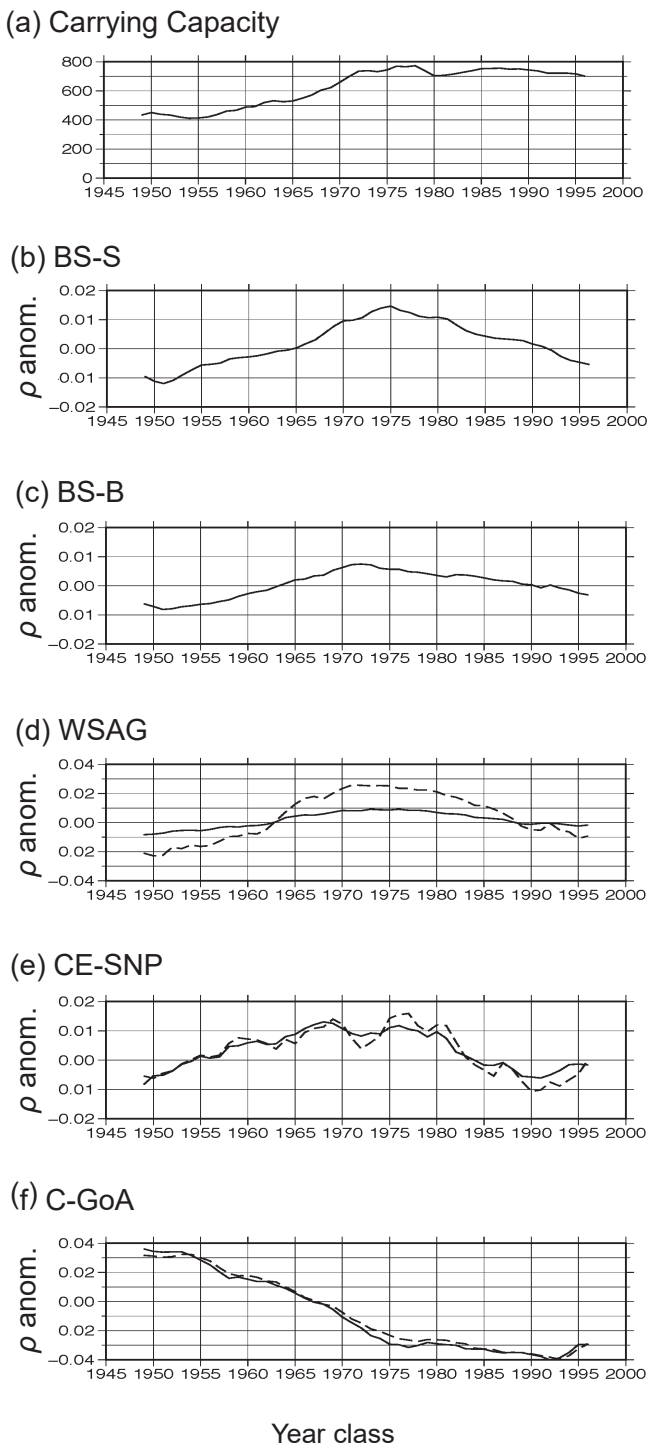

Fig. 5. Temporal changes in (a) carrying capacity (millions of fish) (Kaeriyama et al. 2009) and the ρ anomaly in summer (June–October, solid line) and winter (December–April, dashed line) in (b) BS-S, (c) BS-B, (d) WSAG, (e) CE-SNP, and (f) C-GoA. Values in (b)–(f) are 24-year running means of Fig. 4 (b)–(f) starting from the year class, respectively.

areas BS-S, BS-B, and WSAG are the key areas connecting climate variability and carrying capacity from the perspective of prey density.

DISCUSSION

We discuss the analysis of the relationship between climate variability and prey density in 3D NEMURO (Aita et al. 2007). The temporal and spatial variation in prey (ZP) in 3D NEMURO is related to climate variability via changes in (1) wind strength and pattern, (2) mixed layer depth and Ekman pumping, and (3) primary production (Aita et al. 2007). Stronger westerly winds after the 1976/77 regime shift induced a deeper mixed layer and stronger Ekman upwelling in the central subarctic North Pacific (including the WSAG and CE-SNP in this study), increasing primary production and zooplankton in the WSAG and a very slight increase in the CE-SNP (Aita et al. 2007). In contrast, in the coastal upwelling region of the C-GoA strengthened warm water advection resulted in a reduced mixed layer, causing a decrease in phytoplankton, zooplankton, and primary production (Aita et al. 2007). This mechanism is not consistent with results of other observations (e.g., Polovina et al. 1995) who indicated that zooplankton biomass increased after the mid-1970s because light conditions improved due to a shallower mixed layer. In the Bering Sea, the strengthened Aleutian Low intensified the northerly wind, saline water intruded from the subarctic current, the mixed layer deepened, and primary production increased (Aita et al. 2007). This is also inconsistent with the observed reduction in production (e.g., Sugimoto and Tadokoro 1997).

The inconsistencies in the observations described above are partly caused by the coarse horizontal resolution of the physical model (Aita et al. 2007). However, the lack of top-down control (i.e., predation by fish) in NEMURO might also affect the zooplankton distribution in 3D NEMURO. The ZP used for the estimation of growth condition is the top predator in NEMURO, indicating no predation pressure on ZP. Therefore, ZP density might be considered as the potential prey density for higher-level predators, such as Pacific salmon. From this perspective, it seems reasonable to use the ZP density from NEMURO to investigate the relationship between climate variability and the carrying capacity of Pacific salmon. However, the inclusion of a top-down effect is necessary to investigate the relationship between climate variability and carrying capacity in greater detail.

In this study we focused on the variability in the prey density dependence function for consumption (ρ). We also checked how ρ correlates with the temperature dependence function for consumption ($f_c(T)$). The values were 0.15 in BS-S, -0.32 in BS-B, -0.25 in WSAG, 0.56 in CE-SNP, 0.55 in C-GoA in summer; low in BS-S, BS-B and WSAG, the key areas, suggesting that at least in these areas consumption of Pacific salmon has to be studied from the view point of prey density as well as temperature.

ACKNOWLEDGMENTS

The authors would like to thank Masashi Kiyota for helpful and constructive comments and Masaru Inatsu for supporting EOF analysis. The authors also would like to thank Edward V. Farley, Elizabeth Siddon and an anonymous reviewer for their helpful comments. This study was conducted as a part of NEOPS (New Ocean Paradigm on its Biogeochemistry, Ecosystem and Sustainable Use) supported by a KAKENHI Grant-in-Aid for Scientific Research on Innovative Areas Grant Number 24121008 from the Ministry of Education, Culture, Sports, Science, and Technology of Japan.

REFERENCES

Aita, M.N., Y. Yamanaka, and M.J. Kishi. 2007. Interdecadal variation of the lower trophic ecosystem in the Northern Pacific between 1948 and 2002, in a 3-D implementation of the NEMURO model. Ecol. Model. 202: 81–94.

Beamish, R.J., and D. Bouillion. 1993. Pacific salmon production trends in relation to climate. Can. J. Fish. Aquat. Sci. 50: 1002–1016.

Beauchamp, D.A., D.J. Stewart, and G.L. Thomas. 1989. Corroboration of a bioenergetics model for sockeye salmon. Trans. Am. Fish. Soc. 118: 597–607.

Brodeur, R.D., B.W. Frost, S.R. Hare, R.C. Francis, and W.J. Ingraham, Jr. 1996. Interannual variations in zooplankton biomass in the Gulf of Alaska and covariation with California Current zooplankton. Calif. Coop. Ocean. Fish. Invest. Rep. No. 37: 80–99.

Gargett, A.E. 1997. The optimal stability 'window': A mechanism underlying decadal fluctuations in North Pacific salmon stocks? Fish. Oceanogr. 6: 109–117.

Hare, S.R., N.J. Mantua, and R.C. Francis. 1999. Inverse production regimes: Alaskan and west coast salmon. Fisheries 24: 6–14.

Irvine, J.R., A. Tompkins, T. Saito, K.B. Seong, J.K. Kim, N. Klovach, H. Bartlett, and E. Volk. 2012. Pacific salmon status and abundance trends - 2012 update. N. Pac. Anadr. Fish Comm. Doc. 1422. 90 pp. (Available at www.npafc.org).

Ito, S., M.J. Kishi, Y. Kurita, Y. Oozeki, Y. Yamanaka, B.A. Megrey, and F.E. Werner. 2004. Initial design for a fish bioenergetics model of Pacific saury coupled to a lower trophic ecosystem model. Fish. Oceanogr. 13: 111–124.

Kaeriyama, M., and M. Minagawa. 2008. Effects of anadromous fish on material transportations to the terrestrial ecosystem. *In* Discoveries in aquatic animal ecology presented by stable isotope scope - bivalve to whale. *Edited by* O. Tominaga and N. Takai. Koseisha-Koseikaku, Tokyo. pp. 110–123.

Kaeriyama, M., H. Seo, and H. Kudo. 2009. Trends in run size and carrying capacity of Pacific salmon in the North Pacific Ocean. N. Pac. Anadr. Fish Comm. Bull. 5: 293–302. (Available at www.npafc.org).

Kamezawa, Y., T. Azumaya, T. Nagasawa, and M.J. Kishi. 2007. A fish bioenergetics model of Japanese chum salmon (*Oncorhynchus keta*) for studying the influence of environmental factor changes. Bull. Japan. Soc. Fish. Oceanogr. 71: 87–96. (In Japanese with English abstract).

Kishi, M.J., M. Kashiwai, D.M. Ware, B.A. Megrey, D.L. Eslinger, F.E. Werner, M.N. Aita, T. Azumaya, M. Fujii, S. Hashimoto, D. Huang, H. Iizumi, Y. Ishida, S. Kang, G.A. Kantakov, H. Kim, K. Komatsu, V.V. Navrotsky, S.L. Smith, K. Tadokoro, A. Tsuda, O. Yamamura, Y. Yamanaka, K. Yokouchi, N. Yoshie, J. Zhang, Y.I. Zuenko, and V.I. Zvalinsky. 2007. NEMURO - a lower trophic level model for the North Pacific marine ecosystem. Ecol. Model. 202: 12–25.

Kishi, M.J., M. Kaeriyama, H. Ueno, and Y. Kamezawa. 2010. The effect of climate change on the growth of Japanese chum salmon (*Oncorhynchus keta*) using a bioenergetics model coupled with a three-dimensional lower tropic ecosystem model (NEMURO). Deep-Sea Res. II 57: 1257–1265.

Mantua, N.J., S.R. Hare, Y. Zhang, J.M. Wallace, and R.C. Francis. 1997. A Pacific interdecadal climate oscillation with impacts on salmon production. Bull. Am. Meteorol. Soc. 78: 1069–1079.

Megrey, B.A., K. Rose, F.E. Werner, R.A. Klumb, and D. Hay. 2002. A generalized fish bioenergetics/biomass model with an application to Pacific herring. PICES Sci. Rep. 20: 4–12.

Myers, K.W., N.V. Klovach, O.F. Gritsenko, S. Urawa, and T.C. Royer. 2007. Stock-specific distributions of Asian and North American salmon in the open ocean, interannual changes, and oceanographic conditions. N. Pac. Anadr. Fish Comm. Bull. 4: 159–177. (Available at www.npafc.org).

Polovina, J.J., G.T. Mitchum, and G.T. Evans. 1995. Decadal and basin-scale variation in mixed-layer depth and the impact on biological production in the central and North Pacific, 1960–88. Deep Sea Res. 42: 1701–1716.

Royer, T.C., C.E. Grosch, and L.A. Mysak. 2001. Interdecadal variability of northeast Pacific coastal freshwater and its implications on biological productivity. Prog. Oceanogr. 49: 95–111.

Rudstam, L.G. 1988. Exploring the dynamics of herring consumption in the Baltic: Applications of an energetic model of fish growth. Kieler Meeresforsch. Sonderh. 6: 312–322.

Stachura M.M., N.J. Mantua, and M.D. Scheuerell. 2014. Oceanographic influences on patterns in North Pacific salmon abundance. Can. J. Fish. Aquat. Sci. 71: 226–235

Sugimoto, T., and K. Tadokoro. 1997. Interannual-interdecadal variations in zooplankton biomass, chlorophyll concentration and physical environment in the

subarctic Pacific and Bering Sea. Fish. Oceanogr. 6: 74–93.

Thornton, K.W., and A.S. Lessem. 1978. A temperature algorithm for modifying biological rates. Trans. Am. Fish. Soc. 107: 284–287.

Trudel, M., D.R. Geist, and D.W. Welch. 2004. Modeling the oxygen consumption rates in Pacific salmon and steelhead: An assessment of current models and practices. Trans. Am. Fish. Soc. 133: 326–348.

Ware, D.W. 1978. Bioenergetics of pelagic fish: theoretical change in swimming speed and ration with body size. J. Fish. Res. Board Can. 34: 220–228.

Yoon, S., E. Watanabe, H. Ueno, and M.J. Kishi. 2015. Potential habitat for chum salmon (*Oncorhynchus keta*) in the Western Arctic based on a bioenergetics model coupled with a three-dimensional lower trophic ecosystem model. Prog. Oceanogr. 131: 146–158.